Structures and Energetics of the Cation−π Interactions of Li^+, Na^+, and K^+ with Cup-Shaped Molecules: Effect of Ring Addition to Benzene and Cavity Selectivity

T. C. Dinadayalane,[†] Dmitriy Afanasiev,[†,‡] and Jerzy Leszczynski*[,†]

Computational Center for Molecular Structure and Interactions, Department of Chemistry, Jackson State University, 1400 JR Lynch Street, P.O. Box 17910, Jackson, Mississippi 39217, and Ukrainian State Chemical Technology University, Gagarin av., 8, Dnepropetrovsk, 49005, Ukraine

Received: March 14, 2008; Revised Manuscript Received: June 9, 2008

The interactions of alkali metal cations (Li^+, Na^+, and K^+) with the cup-shaped molecules, tris(bicyclo[2.2.1]-hepteno)benzene and tris(7-azabicyclo[2.2.1]hepteno)benzene have been investigated using MP2(FULL)/6-311+G(d,p)//MP2/6-31G(d) level of theory. The geometries and interaction energies obtained for the metal ion complexation with the cup-shaped systems trindene and benzotripyrrole are compared with the results for benzene−metal ion complexes to examine the effect of ring addition to the benzene on structural and binding affinities. The cup-shaped molecules exhibit two faces or cavities (top and bottom). Except for one of the conformers of tris(7-azabicyclo[2.2.1]hepteno)benzene), the metal ions prefer to bind with the top face over bottom face of the cup-shaped molecules. The selectivity of the top face is due to strong interaction of the cation with the π cloud not only from the central six-membered ring but also from the π electrons of rim C=C bonds. In contrast, the metal ions under study exhibit preference to bind with the bottom face rather than top face of tris(7-azabicyclo[2.2.1]hepteno)benzene) when the lone pair of electrons of three nitrogen atoms participates in binding with metal ions. This bottom face selectivity could be ascribed to the combined effect of the cation−π and strong cation−lone pair interactions. As evidenced from the values of pyramidalization angles, the host molecule becomes deeper bowl when the lone pair of electrons of nitrogen atoms participates in binding with cation. Molecular electrostatic potential surfaces nicely explain the cavity selectivity in the cup-shaped systems and the variation of interaction energies for different ligands. Vibrational frequency analysis is useful in characterizing different metal ion complexes and to distinguish top and bottom face complexes of metal ions with the cup-shaped molecules.

Introduction

Structures and biochemical functions of biological systems are controlled by noncovalent interactions such as hydrogen bonds, salt bridges, and hydrophobic, cation−π, charge-dipole, and π-stacking interactions.[1,2] Noncovalent intermolecular interactions involving π-systems have been receiving a great deal of attention because of their importance in molecular recognition, designing molecular materials with desirable physicochemical properties, elucidation of enzymatic reaction mechanisms, design of nanomaterials, ion-selective ionophores, and receptors.[3] The cation−π interaction, which occurs between cations and π-systems, is generally stronger than that of other nonbonding interactions involving π-systems.[2,4] The cations involved in such interactions may comprise metal cations as well as complex organic cations, while the π-system can vary from a simple π-system (e.g., ethylene) to complex single and multiple aromatic ring systems. The cation−π interactions have been a fascinating topic in many areas of chemistry, biology, biophysics, molecular biology, and material science.[2–9] The nature of cation−π interactions and their role in biological systems were widely appreciated after the pioneering work of Dougherty and co-workers.[1,2] Although cation−π interactions have been known for three decades,[10] they have been recognized very well as an important noncovalent interaction only in recent years.[11–19] The interactions of cations with the aromatic rings of the amino acids are of the current theoretical interests.[18,19]

Kim and co-workers demonstrated that [n]collarenes can be used as efficient ionophores, which form complexes with cations via cation−π interactions, because of their structural rigidity and well-defined cavity size.[20] Cage-type molecules possess structurally well-defined cavities. They are given special interest due to their paramount importance in supramolecular chemistry, particularly cation−π interactions. Binding of ammonium and alkali metal cations (Li^+, Na^+ and K^+) with the cage-type molecules possessing π-cavity through cation−π interactions has been studied experimentally, in the gas phase.[21] A recent experimental study of Bartsch and co-workers has shown that calix[4]arene derivatives using crown ethers are useful for solvent extraction of alkaline earth metal cations from water into chloroform.[22] The synthesis of cup-shaped molecules of benzotri(benzonorbornadienes) that possess high electron density within the cavity has been reported. Furthermore, these molecules accommodate fullerene C_{60} in the cavity.[23] Very similar cup-shaped molecules are considered in this paper to examine their binding affinity with alkali metal cations. The cup-shaped molecules exhibit a rigid geometry with π-cavities, which can be useful for alkali and alkaline earth metal cation extractions through cation−π interactions. Thus, they could be used as effective ionophores and molecular receptors and could have practical applications in environmental chemistry and biology.

Numerous experimental studies have been reported for cation−π interactions of several model systems in the gas

* To whom correspondence should be addressed. E-mail: jerzy@ccmsi.us.
† Jackson State University.
‡ Ukrainian State Chemical Technology University.

10.1021/jp802236k CCC: $40.75
Published on Web 08/02/2008

SCHEME 1

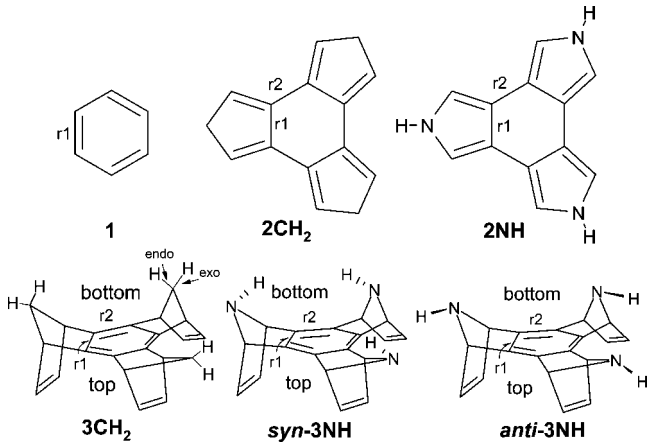

phase.[11,21,22,24–27] Theoretical calculations have complemented the experimental results for various model systems.[10,11,24–28] The influence of electron-donating and electron-withdrawing substituents attached to the aromatic ring, particularly benzene, on cation$-\pi$ interactions has been studied by both experimentalists and theoreticians.[2,5,6,11,12,24–28] Some of the computational studies have focused their investigations toward understanding the origin of the cation$-\pi$ interaction energies by partitioning them into different energy components such as electrostatic, induction, exchange repulsion, dispersion, etc.[14,28] Recently, interactions of various cations with arenes and heteroarenes of five- and six-membered cyclic systems have been explored to obtain the knowledge on the cation$-\pi$ interactions in the heteroaromatic systems.[14,15]

The effect of increasing the size of the π network of cyclic and acyclic systems on the cation$-\pi$ interaction energies has been demonstrated.[29–32] Investigations involving interactions of cations with the planar and curved polycyclic systems have been reported.[33,34] Calixarene-based ligands for complexation with metal ions have received widespread interest due to their high extraction efficiencies and selectivities for metal ions.[22,35,36] Although synthesis and structures of the cup-shaped tris-annulated benzenes have been reported,[23,37,38] the studies concerning the metal ion binding with their π-cavity are scarce. We have recently reported that the ring annulation to benzene has significant influence on Li^+ binding affinity, vibrational frequencies, and NMR chemical shifts.[39]

In the present paper, we have investigated the interactions of the alkali metal cations (Li^+, Na^+, and K^+) with the cup-shaped molecules of tris(bicyclo[2.2.1]hepteno)benzene and tris(7-azabicyclo[2.2.1]hepteno)benzene. We have also carried out the calculations for the interactions of the above-mentioned metal ions with benzene, trindene, and benzotripyrrole. This comprehensive study provides knowledge on the effect of fusing mono- and bicyclic rings to benzene on the strength of cation$-\pi$ interactions. The host molecules for alkali metal ion binding considered in this study are shown in Scheme 1. The synthesis of cup-shaped molecules has stimulated our interest to carry out the systematic theoretical study of cation$-\pi$ interactions.[23,37,38] We intend to address the following questions: (a) Which face of the cup-shaped molecule is preferred (either top or bottom face) for the metal ion complexation? (b) Is the face selectivity same for all the three metal ions considered? (c) How does the geometry of the cup-shaped molecule change upon the complexation with the metal cation? (d) How does the binding affinity of the metal ions vary by fusing mono- and bicyclic rings to the benzene?

Computational Details

The structures of all the ligands and the alkali metal ion-bound complexes were initially optimized at the hybrid density functional, B3LYP[40] in conjunction with 6-31G(d) basis set. The geometries of all the structures were also optimized at the second-order Møller−Plesset perturbation (MP2)[41] method using the 6-31G(d) basis set. The geometry optimizations for all of the structures were done within the symmetry constrains. Single-point calculations were performed at the MP2(FULL)/6-311+G(d,p) level using MP2/6-31G(d) optimized geometries. The interaction energy was determined from the difference between the total energy of the complexes and the sum of the total energies of the corresponding isolated cation and ligand. The correction for basis set superposition error (BSSE) for all of the complexes was carried out using the counterpoise (CP) method of Boys and Bernardi.[42] The extent of electron charge transfer from the ligand to alkali metal ion (q_{CT}), which is the difference between the actual charge of the metal ion (+1 for the alkali metal ions) and its residual charge in the complex, was calculated using charges from the natural population analysis (NPA) at all three levels considered in this study. The BSSE corrected interaction energies and the extent of electron charge transfer from the ligand to alkali metal ion (q_{CT}) obtained at the MP2(FULL)/6-311+G(d,p) level are presented in the paper, and the results obtained using B3LYP/6-31G(d) and MP2/6-31G(d) levels are provided in the Supporting Information.

Vibrational frequency calculations at the MP2/6-31G(d) level for the complexes involving cup-shaped molecules are not viable within our current computational resources. Therefore, we have performed frequency calculations at the B3LYP/6-31G(d) level for all of the ligands and complexes to ascertain that the structures are minima on their respective potential energy surfaces. We have also reported the important frequencies of the ligands and their metal ion complexes. Molecular electrostatic potential (MEP) surfaces for all of the ligands under study were generated using the electron density at the MP2/6-31G(d) level. The pictures of MEP surfaces for the ligands were obtained using Gaussview 3.09.[43] All of the calculations were performed using Gaussian 03 suit of programs.[44] The pyramidalization angle (θ_P) at the carbon atom of the central six-membered ring of the annulated systems and their metal ion-bound complexes was estimated using Haddon's π-orbital axis vector (POAV) angles.[45,46] Haddon developed π-orbital axis vector (POAV) analysis to describe the distortions of double bonds. The π-orbital axis vector is defined as that vector which makes equal angles ($\theta_{\sigma\pi}$) to the three σ-bonds at a conjugated carbon atom, and the pyramidalization angle is obtained as $\theta_P = (\theta_{\sigma\pi} - 90)°$.[45] The pyramidalization angle is an useful quantity to gauge the deviation from the planarity of the carbon atoms in the nonplanar conjugated organic molecules for, e.g., bridged annulenes and fullerenes.

Results and Discussion

Structures of Ligands and Complexes. Scheme 1 depicts the ligands of benzene (**1**), triphenylene (**2CH$_2$**), benzotripyrrole (**2NH**), tris(bicyclo[2.2.1]hepteno)benzene (**3CH$_2$**) and tris(7-azabicyclo[2.2.1]hepteno)benzene (***syn-*** and ***anti*-3NH**) for complexation with alkali metal ions. The compounds **2CH$_2$** and **2NH** are planar. They contain three monocyclic rings fused to alternate sides of benzene, whereas the bicyclic rings are fused to benzene in ligands **3CH$_2$**, ***syn*-3NH** and ***anti*-3NH** that are called cup-shaped molecules. The nomenclature of ***syn*-3NH** and ***anti*-3NH** is given based on the orientation of the N−H bonds. The prefixes syn and anti are used to represent all three

TABLE 1: MP2/6-31G(d) Level Bond Distances (in Å) of endo (r_1) and exo (r_2) Bonds and the Bond Length Alternation (Δr) for the Ring Fused Benzene Ligands and Their Metal Ion-Bound Complexes[a]

	ligand			ligand−Li^+			ligand−Na^+			ligand−K^+		
ligand name	r_1	r_2	Δr	r_1	r_2	Δr	r_1	r_2	Δr	r_1	r_2	Δr
1	1.397			1.406			1.404			1.402		
2CH$_2$	1.481	1.457	0.024	1.490	1.464	0.026	1.488	1.463	0.025	1.486	1.461	0.025
2NH	1.435	1.447	−0.012	1.446	1.454	−0.008	1.443	1.454	−0.011	1.440	1.451	−0.011
3CH$_2$	1.421	1.379	0.042	1.435 (1.432)	1.390 (1.385)	0.045 (0.047)	1.431 (1.428)	1.388 (1.384)	0.043 (0.044)	1.427 (1.425)	1.385 (1.383)	0.042 (0.042)
***syn*-3NH**	1.426	1.374	0.052	1.440 (1.438)	1.386 (1.379)	0.054 (0.059)	1.437 (1.434)	1.384 (1.378)	0.053 (0.056)	1.432 (1.431)	1.382 (1.377)	0.050 (0.054)
***anti*-3NH**	1.421	1.373	0.048	1.431 (1.435)	1.376 (1.377)	0.055 (0.058)	1.429 (1.431)	1.374 (1.375)	0.055 (0.056)	1.427 (1.428)	1.373 (1.375)	0.054 (0.053)

[a] The C−C bond distance of benzene and its complexes are also given for comparison. The values given in parentheses correspond to the complexes wherein the metal ion is bound with the top face.

N−H bonds projecting inward (toward the central benzene ring) and projecting outward (away from the central benzene ring), respectively. One can anticipate the involvement of lone pair of electrons of nitrogen atoms on binding with alkali metal ions together with cation−π interactions in the case of ***anti*-3NH**. Therefore, both ***syn*-3NH** and ***anti*-3NH** are considered in this study. It is pertinent to note that ***syn*-3NH** is slightly more stable (∼0.5 kcal/mol) than ***anti*-3NH**. In the cup-shaped molecules, there are two different faces (or cavities) for the metal ion binding. The side with three CH_2 or NH bridges is named as the bottom face, whereas the other side that consists of three rim C═C bonds is considered as top face. The selectivity of the face for the alkali metal ion binding with the cup-shaped molecules is the primary focus of this study. The reasons for the selectivity of the top or bottom face of the cup-shaped molecules will be discussed.

In the ligand **3CH$_2$**, as shown in Scheme 1, the C−H bond of bridge CH_2 projecting toward central six-membered ring (inward) is named as the endo C−H bond, whereas the other C−H bond projecting away from the central six-membered ring (outward) is named as the exo C−H bond. It is expected that the endo C−H bond may be affected when the metal ions bind through the bottom face. In the case of ***syn*-3NH**, the N−H bond may play a role in the metal ion complexation via the bottom face. The metal ion complexation with the top face of cup-shaped ligands may influence the C−H bond length and the stretching frequency of rim H−C═C−H. Therefore, the bond lengths and the stretching frequencies associated with them are provided and examined in the latter section of vibrational frequency analysis.

Addition of mono- and bicyclic rings to the benzene leads to bond alternation or localization, which is associated with the Mills−Nixon effect.[47] Nearly 80 years ago, Mills and Nixon postulated that the fusion of a small ring to the benzene molecule induces π-bond localization in the benzene ring. This phenomenon is so-called the Mills−Nixon effect.[47] As reported in earlier studies, the C−C bond, which is shared by the benzene and fused ring, is the endo C−C bond (bond length, r_1), whereas the unshared C−C bond of the benzene is named as exo C−C bond (bond length, r_2) (Scheme 1). In this study, we have analyzed the changes in the bond lengths of both the endo and exo C−C bonds upon metal ion binding. All of these ring fused benzenes and their alkali metal ion complexes possess trigonal symmetry. Except for the benzene systems, all of the complexes are characterized by the C_{3v} point group.

The bond lengths of endo (r_1) and exo (r_2) bonds and the bond length alternation ($\Delta r = r_1 - r_2$) obtained at the MP2/6-31G(d) level for the ring fused benzene ligands and their metal ion-bound complexes are listed in Table 1. The C−C bond distance of **1** and its complexes obtained at the MP2/6-31G(d) level exhibits negligible deviation (∼0.002 Å) compared to the MP2/6-311+G(d) level geometries reported by Nicholas et al.[48] The C−C bond distances of 1.421 Å (endo, r_1) and 1.379 Å (exo, r_2) obtained for **3CH$_2$** at the MP2/6-31G(d) level are in excellent agreement with the X-ray crystallographic bond lengths of 1.422 and 1.379 Å for a very similar compound of tris-norbornabenzene.[49] This agreement supports the adequacy of the MP2/6-31G(d) level for the geometries of ring fused benzene systems. Similar to the prototype benzene system, the C−C bonds of the central hexagon in ring fused benzenes undergo elongation upon complexation with the alkali metal ions. A straightforward interpretation for the elongation of the C−C bonds would be the donation of electron charge from the ligand to the metal ion. Binding of Li^+ with the ligands lengthens the C−C bonds of the central six-membered ring to the maximum extent, whereas the interaction of K^+ with the same ligand yields the least elongation of the C−C bond lengths. Thus, the lengthening of the C−C bond is less pronounced as the size of the cation increases.

As shown in Table 1, the bond lengths of both endo and exo C−C bonds of **2CH$_2$**, **2NH**, and their metal ion complexes are significantly longer compared to the cup-shaped ligands and their complexes. However, the degree of bond alternation is much higher in the cup-shaped systems and their metal ion complexes. This can be interpreted as a consequence of geometric distortion induced by fusing bicyclic rings to the benzene. In the case of **2NH** and its complexes, the endo bond distance is notably shorter than the exo bond length. Hence, we obtained negative values for bond length alternation. The ligand **2CH$_2$** and its complexes, wherein the fused rings are nonaromatic, show significant bond length alternation, whereas the least bond alternation is observed for **2NH** and its metal ion complexes because of the participation of lone pair of electrons of nitrogen in delocalization. Thus, the electronic factor influences the bond alternation. It is imperative to point out that the bond length alternation is enhanced by the binding of alkali metal ions. This can be ascribed to the donation of electron density from the central ring to the metal ion and the geometric distortion induced by the metal ion binding. In general, the bond length alternation decreases with an increase in the metal ion size in the complexes. For the cup-shaped ligands **3CH$_2$** and ***syn*-3NH**, the alkali metal ion binding to the bottom face yields marginally higher elongation of both the endo and exo C−C bonds of the central six-membered ring compared to the metal ion interaction with the top face. However, the complexes formed via the bottom face exhibit slightly smaller bond length alternation than those formed through the top face. The situation for ***anti*-3NH** is in sharp contrast to **3CH$_2$** and ***syn*-3NH**.

The MP2/6-31G(d) level optimized structures of the complexes that are formed by the binding of alkali metal ions with the ligands **1**, **2CH$_2$**, and **2NH** are depicted in Figure 1. The selected geometric parameters of the complexes formed by the

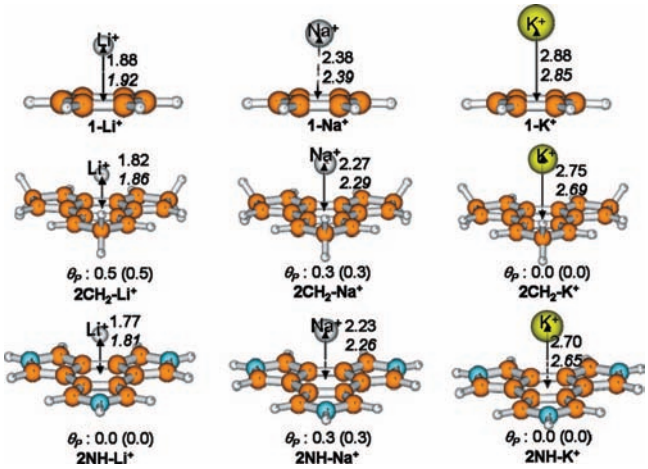

Figure 1. MP2/6-31G(d) optimized structures of the cation−π complexes of alkali metal ions (Li^+, Na^+, and K^+) with π-systems of benzene (**1**), trindene (**2CH$_2$**), and benzotripyrrole (**2NH**). The distance (in Å) between the metal ion and the center of hexagon of the ligands obtained at the B3LYP/6-31G(d) (plain) and MP2/6-31G(d) (italics) levels, and also given the pyramidalization angle (θ_P, in degrees) at the carbon atom of the hexagon of the complexes optimized at the B3LYP/6-31G(d) and MP2/6-31G(d) (in parenthesis) levels.

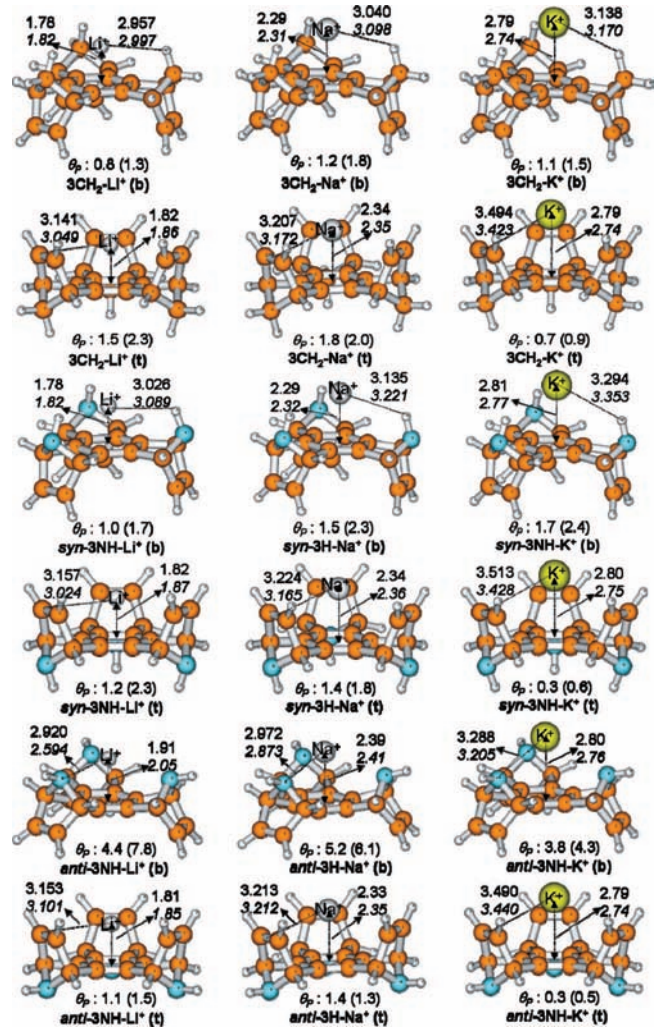

Figure 2. Principal geometric parameters obtained at the B3LYP/6-31G(d) (plain) and MP2/6-31G(d) (italics) levels for the complexes formed by Li^+, Na^+, and K^+ with the cup-shaped molecules. The pyramidalization angle (θ_P, in degrees) at the carbon atom of the hexagon of the complexes optimized at the B3LYP/6-31G(d) and MP2/6-31G(d) (in parenthesis) levels.

binding of metal ions with the cup-shaped ligands are shown in Figure 2. In the nomenclature, the letters **(b)** and **(t)** are used to represent the metal ion binding with the bottom and top faces of the cup-shaped molecule, respectively. In the case of metal ion binding with the top face, the distance between the metal ion and the center of rim C=C is also provided in Figure 2. We have evaluated the pyramidalization angle, which gauges the deviation of planarity of the sp^2 hybridized carbon in the curved polycyclic systems, at the carbon atom of the central six-membered ring of the complexes involving ring-fused benzene ligands and the values are given in Figures 1 and 2. As expected, the distance between the metal ion and the centroid of the hexagon of ligand increases as the atomic radius of the metal increases. In comparison with the prototype benzene−alkali metal ion complexes, the M^+−centroid distance considerably decreases for the ligands involving **2CH$_2$** and **2NH**. Indeed, the complexes involving the latter ligand exhibit notably shorter distance compared to the former ligand. In general, the B3LYP/6-31G(d) level predicts a shorter intermolecular distance of the M^+−centroid compared to the MP2/6-31G(d) level for the complexes involving Li^+ and Na^+ ions, while the situation is exactly opposite for the complexes involving K^+ ion. The MP2 geometries are taken for discussion in the rest of the section unless otherwise specified. Very small (less than 1°) pyramidalization angle obtained for the complexes **2CH$_2$-Li$^+$**, **2CH$_2$-Na$^+$**, and **2NH-Na$^+$** indicates that the carbon atoms of the central six-membered ring deviate from the planarity to a slight pyramidal shape. The host molecules are essentially planar in the complexes of **2CH$_2$-K$^+$**, **2NH-Li$^+$**, and **2NH-K$^+$**.

In general, the M^+−centroid distance is shorter in both the bottom and top face complexes than in the corresponding benzene complexes, indicating that fusing of bicyclic rings to the benzene decreases the distance between the metal ion and the ring centroid. Figure 2 shows that the bottom face complexes exhibit a shorter M^+−centroid distance compared to the top face complexes involving **3CH$_2$** and ***syn*-3NH** only if the metal ion is Li^+ or Na^+. The situation is opposite in the complexes involving ***anti*-3NH** because of the interaction of the lone pair electrons of nitrogen atoms with the metal ion in the bottom face complexes. For the same reason, the fused rings move upward toward the cation in the bottom face complexes of ***anti*-3NH**, which is apparent from the optimized geometries and the substantially high pyramidalization angles (Figure 2). The structures shown in Figure 2 indicate that alkali metal ion binding with the bottom face of **3CH$_2$** and ***syn*-3NH** causes the fused bicyclic rings to move downward (away from the cation). The carbon atoms of the central six-membered ring skeleton of the cup-shaped ligands are planar as evidenced from a value of zero for the pyramidalization angles. They deviate from planar to pyramidal carbon upon complexation with the alkali metal ions. The optimized structures of the complexes and the values of the pyramidalization angles indicate that the fused bicyclic rings undergo up or down flexible movement when the metal ion binds with the bottom or top face of the ligand. For all of the three cup-shaped ligands, the binding of Li^+ with the top face leads to higher pyramidalization of the carbon of the central hexagon compared to Na^+ and K^+ complexes.

Energetics and Charge Transfer. The BSSE corrected interaction energies obtained at the MP2(FULL)/6-311+G(d,p) level along with the extent of electron charge transfer from the ligand to the metal ion for all of the complexes are listed in Table 2. For the benzene system, the computed interaction energies are in good agreement with the experimental values.[25]

TABLE 2: BSSE Corrected Interaction Energies (ΔE, in kcal/mol) and the Extent of Electron Charge Transfer from Ligand to Metal Ion (q_{CT}, e$^-$) using NPA Charges Calculated at the MP2(FULL)/6-311+G(d,p) Level

		MP2(FULL)/6-311+G(d,p)[b]		
system/complexes[a]		Li^+	Na^+	K^+
1	ΔE	−35.4	−21.4	−16.9
	expt[c]	−38.5 ± 3.2	−22.1 ± 1.4	−17.5 ± 1.0
	q_{CT}	0.050	0.024	0.011
$2CH_2$	ΔE	−38.7	−27.5	−24.2
	q_{CT}	0.035	0.015	0.004
2NH	ΔE	−57.9	−41.8	−36.2
	q_{CT}	0.045	0.019	0.011
$3CH_2$ (b)	ΔE	−50.7	−31.4	−25.4
	q_{CT}	0.062	0.029	0.019
$3CH_2$ (t)	ΔE	−55.3	−39.0	−33.9
	q_{CT}	0.093	0.062	0.034
***syn*-3NH (b)**	ΔE	−39.2	−20.3	−14.7
	q_{CT}	0.061	0.028	0.016
***syn*-3NH (t)**	ΔE	−47.0	−31.5	−27.1
	q_{CT}	0.101	0.066	0.037
***anti*-3NH (b)**	ΔE	−61.1	−49.4	−45.0
	q_{CT}	0.117	0.070	0.041
***anti*-3NH (t)**	ΔE	−49.7	−33.0	−28.3
	q_{CT}	0.089	0.058	0.034

[a] The nomenclature **(b)** and **(t)** represent the metal ion complexation with the bottom and top face of the ligand respectively. [b] Single-point calculations were performed on the MP2/6-31G(d) optimized geometries. [c] Experimental ΔH values taken from ref 25.

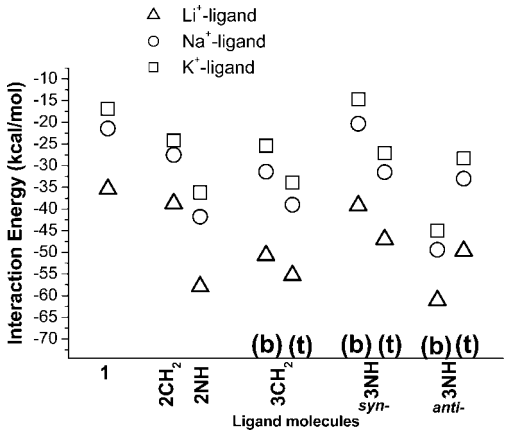

Figure 3. Variation of interaction energies obtained at the MP2(FULL)/6-311+G(d,p)//MP2/6-31G(d) level for the metal ion binding with a range of ligands. In the nomenclature, **(b)** and **(t)** represent the metal ion binding with the bottom and top face of the cup-shaped ligands.

Figure 3 illustrates the variation of interaction energies when different metal ions interact with a series of ligands considered in this study. For all of the ligands, Li^+ binds stronger than Na^+ and K^+ ions due to a strong electrostatic interaction. Similar to benzene, the binding affinity of the metal ion with each of the ring fused benzenes follows the order $Li^+ > Na^+ > K^+$. A charge−dipole interaction is responsible for the binding of cations with the cup-shaped molecules, whereas a charge−polarization effect plays an important role in binding of metal ions with the planar ligands. In comparison with benzene (**1**), the binding affinity of alkali metal ions with **$2CH_2$** and **2NH** is significantly enhanced. We observe that the binding affinity of metal ions with **2NH** is substantially stronger than with **$2CH_2$**. It is imperative to mention that electron delocalization occurs in the former ligand, whereas there is no electron delocalization in **$2CH_2$** wherein the antiaromatic five-membered rings are fused to benzene. Thus, the electron delocalization over the whole molecule has a significant effect on the strength of interaction. In line with the binding strength, the M^+−centroid distance is shorter in the complexes involving **2NH** than in **$2CH_2$** (Figure 1). As shown in Table 2, the extent of electron charge transfer from ligand to metal ion is lower in the complexes involving **$2CH_2$** and **2NH** compared to benzene−metal ion complexes. However, the extent of electron charge transfer from **2NH** to metal ion is larger compared to those from **$2CH_2$** to respective metal ion, in agreement with the interaction energies.

Figure 3 clearly shows that the metal ions prefer to bind with the top face rather than bottom face of **$3CH_2$** and ***syn*-3NH**. The metal ion binding strength is decreased when we move from **$3CH_2$** to ***syn*-3NH** in both bottom and top face. The binding of metal ions with the top face of ***syn*-3NH** is more favorable by 8 (Li^+), 11 (Na^+), and 12 (K^+) kcal/mol compared to the bottom face. The top face preference of metal ion binding with **$3CH_2$** and ***syn*-3NH** can be attributed to multiple cation−π interactions. In contrast to **$3CH_2$** and ***syn*-3NH**, the bottom face is more favorable over the top face for the metal ion binding with the ***anti*-3NH**. For the latter ligand, both bottom and top faces have an opportunity for multiple binding with the metal ions. The ligand ***anti*-3NH** allows an effective interaction of lone pair of electrons of three nitrogen atoms with the metal ion in addition to the cation−π interaction when the metal ion binds via the bottom face. The present study reveals that the interactions of cations with the lone pair electrons of three nitrogen atoms prevail over cation−π interactions with three rim C=C bonds. Hence the bottom face is preferred over the top face for the ***anti*-3NH**. As pointed out earlier, the metal ion binding with the bottom face of ***anti*-3NH** induces the bicyclic rings to move upward toward metal ion in order to effectively interact with the lone pair of electrons of three nitrogen atoms (Figure 2). The interaction energies for the metal ion binding with the bottom face of ***anti*-3NH** are the highest among different ligands considered in this study. The computed interaction energies are −61.1 (Li^+), −49.4 (Na^+), and −45.0 (K^+), which are 1.73, 2.31, and 2.66 times that of the corresponding benzene−metal ion complexes.

The bond lengths of rim C=C bonds are 1.347, 1.344, and 1.347 Å for **$3CH_2$**, ***syn*-3NH**, and ***anti*-3NH**, respectively. These bond lengths are virtually unaltered when the metal ions interact with the bottom face of the ligands. Nevertheless, the above-mentioned bond lengths elongated to 1.352, 1.349, and 1.351 Å irrespective of the metal ions interacting with the top face of the cup-shaped ligands. Such an elongation (at least 0.004 Å) of the rim C=C bond length supports the existence of weak cation−π interactions with the rim C=C bonds in the top face complexes. Thus, the interactions of metal ions with the top face of the cup-shaped molecules involve not only the cation−π interaction with the π-cloud of the central six-membered ring but also the weak cation−π interactions with three rim C=C bonds. The present study highlights the important contributions of multiple weak cation−π interactions to the overall binding strength when the metal ions interact via the top face of the cup-shaped molecules.

It is interesting to observe that the binding strengths of Na^+ and K^+ with the bottom face of ***syn*-3NH** are substantially lower compared to benzene (**1**). However, ***syn*-3NH** binds Li^+ to its bottom face stronger (∼4 kcal/mol) than benzene (**1**). As shown in Figure 2, the smaller Li^+ ion fits inside the bottom cavity of ***syn*-3NH** where it experiences less repulsion with the N−H bonds, whereas the larger Na^+ and K^+ ions do not fit inside the bottom cavity thus undergo repulsive interactions with the electropositive hydrogen atoms of bridge N−H. It is pertinent

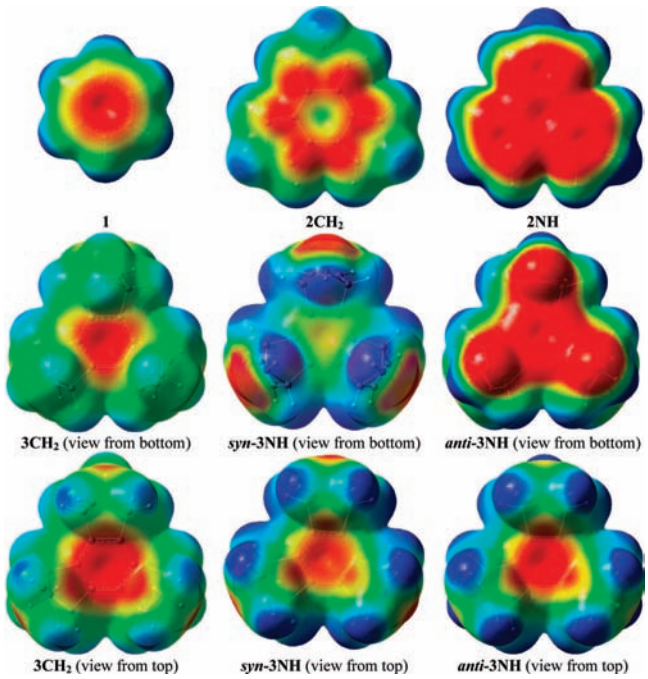

Figure 4. Molecular electrostatic potential maps generated using density at the MP2/6-31G(d) level for benzene and symmetrical triannelated benzene frameworks considered in this study. Electrostatic potentials are mapped on the surface of the electron density of the 0.002 unit. The red surface corresponds to a negative region of the electrostatic potential (−0.029 au), whereas the blue color corresponds to region where the potential is positive (+0.029 au).

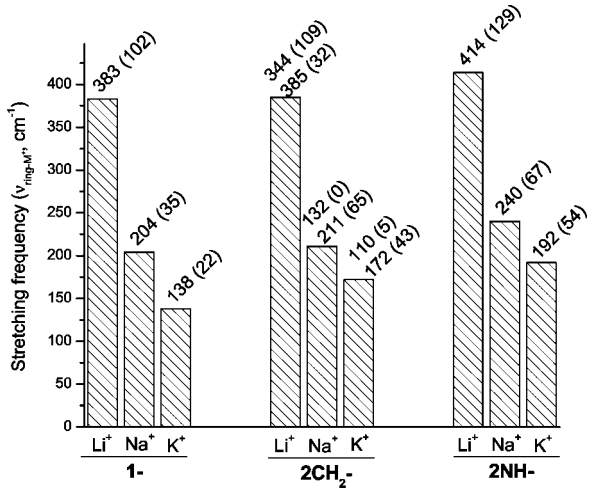

Figure 5. Frequencies of intermolecular stretching mode ($\nu_{\text{ring centroid-M+}}$) for the complexes of Li^+, Na^+, and K^+ with **1**, **2CH$_2$**, and **2NH**.

TABLE 3: Selected C−H and N−H Bond Lengths (in Å) That Are Affected by Metal Ion Interaction, Obtained at the B3LYP/6-31G(d) Level for the Cup-Shaped Molecules

			Li^+ complex		Na^+ complex		K^+ complex	
		ligand	bottom	top	bottom	top	bottom	top
3CH$_2$	endo C−H	1.096	1.100	1.095	1.101	1.095	1.102	1.095
	exo C−H	1.095	1.092	1.093	1.092	1.093	1.093	1.093
	C−H at rim	1.085	1.084	1.085	1.084	1.086	1.084	1.086
***syn*-3NH**	N−H	1.025	1.025	1.024	1.025	1.024	1.026	1.024
	C−H at rim	1.083	1.083	1.084	1.083	1.084	1.083	1.085
***anti*-3NH**	N−H	1.025	1.025	1.023	1.025	1.023	1.025	1.023
	C−H at rim	1.084	1.083	1.085	1.083	1.086	1.083	1.086

to remark that the binding strength of alkali metal ions with the bottom face of ***syn*-3NH** is almost 11 kcal/mol lower compared to those of **3CH$_2$**. This could be ascribed to the strong repulsive interactions between the metal ion and the hydrogen atoms of N−H bonds since the hydrogen atom of N−H bears more positive charge than the endo H-atom of bridge CH_2.

The interaction energies for the metal ion binding with the top face of ***anti*-3NH** are −49.7 (Li^+), −33.0 (Na^+), and −28.3 (K^+). The binding strength is decreased by 2.7, 1.5, and 1.2 kcal/mol correspondingly for the interaction of Li^+, Na^+, and K^+ with the top face of ***syn*-3NH**. Very similar geometrical data for the top face complexes of ***syn*-** and ***anti*-3NH** shown in Figure 2 substantiate these marginal changes in the interaction energies. As expected, the structure of ***anti*-3NH** enables the lone pair of electrons of all three nitrogen atoms to interact with the metal ion via the bottom face, but such an option is prevented in ***syn*-3NH**. Thus, the N−H orientation, which differs in ligands ***syn*-** and ***anti*-3NH**, influences the face selectivity for the metal ion binding, but it does not significantly affect the binding strength of metal ions with the top face. The binding affinity of the metal ion with the top face of **3CH$_2$** is much higher compared to those of ***syn*-** and ***anti*-3NH**. Thus, the present study reveals that the electronic factor significantly influences the strength of metal ion binding.

Previous studies have pointed out that the binding of cations with various π-systems can be explained by charge transfer from π-system to metal ion.[14,29,50] It can be seen from Table 2 that the charge transfer values are much higher for complexes of cup-shaped systems compared to complexes involving **1**, **2CH$_2$**, and **2NH**. The electron charge transfer from ligand to metal ion results in a slight weakening of all of the C−C bonds of the aromatic rings as evidenced from the data given in Table 1. The extent of electron charge transfer is considerably larger for the complexes involving Li^+ compared to Na^+ or K^+. This explains larger elongation of C−C bonds of the central six-membered ring of Li^+ complexes compared to Na^+ and K^+ complexes. For all of the ligands, the value of electron charge transfer from ligand to metal ion decreases as the atomic radius of the metal ion increases. This correlates well with the interaction energies. In agreement with the interaction energies, the electron charge transfer from ligand to metal ion for top face complexes is higher than the bottom face in the cases of **3CH$_2$** and ***syn*-3NH**, whereas the bottom face complex shows higher charge transfer than top face complex in the case of ***anti*-3NH**, irrespective of the metal ion binding with the ligand.

Molecular Electrostatic Potential Surface

Molecular electrostatic potential (MEP) surfaces for all of the ligands are depicted in Figure 4. Two views, bottom and top side view, are shown for the cup-shaped molecules to understand and explain the face selectivity for metal ion binding in such systems. Supramolecular properties of tweezers that possess two different cavities (very similar to cup-shaped molecules) have been studied using electrostatic potential surfaces (EPSs) with semiempirical calculations.[51] The electron density for the MEP surfaces in our study was obtained at the MP2/6-31G(d) level. An electron density isosurface was constructed for each of the ligands, and then the MEP was mapped onto the calculated electron density isosurface of 0.002 eÅ^{-3}. The MEP surfaces were generated using the Gaussview program.[43] For the surfaces, the color code from red to blue was established representing a range of values from −0.029 to +0.029 au, respectively. The dark red and blue colors correspond to the regions of maximum negative and positive potentials.

A quick look at Figure 4 indicates that the electron density at the central benzene ring is much higher in **2NH** than in **2CH$_2$**.

TABLE 4: Important Vibrational Frequencies (cm^{-1}) and Intensities (km/mol) Obtained at the B3LYP/6-31G(d) Level for the Cup-Shaped Ligands ($3CH_2$, syn-3NH, and anti-3NH) and Their Alkali Metal Ion (Li^+, Na^+, and K^+) Complexes[a]

		ligand		ligand−Li^+		ligand−Na^+		ligand−K^+	
system /ligand	description of the frequency	frequency	intensity	frequency	intensity	frequency	intensity	frequency	intensity
$3CH_2$	M^+-central benzene ring intermolecular stretching			413 (394)	61 (50)	215 (199)	33 (21)	150 (150)	26 (18)
	C−H stretching of bridge CH_2	3068	21	3031 (3089)	2 (4)	3011 (3089)	2 (7)	3001 (3087)	2 (7)
		3069	88	3032 (3089)	166 (47)	3013 (3090)	241 (45)	3003 (3088)	317 (51)
		3123	57	3148 (3153)	16 (14)	3142 (3150)	18 (18)	3137 (3147)	20 (22)
		3124	21	3148 (3154)	4 (7)	3142 (3151)	5 (10)	3137 (3148)	6 (10)
	C−H stretching of rim H−C═C−H	3213	10	3237 (3221)	0 (1)	3235 (3211)	1 (2)	3234 (3206)	1 (3)
		3238	14	3258 (3243)	2 (2)	3257 (3233)	3 (3)	3256 (3230)	3 (5)
		3238	42	3259 (3243)	4 (6)	3257 (3234)	6 (11)	3256 (3230)	8 (17)
***syn*-3NH**	M^+-central benzene ring intermolecular stretching			410 (397)	35 (33)	216 (197)	16 (19)	142 (146)	20 (14)
	N−H stretching of bridge NH	3417	3	3409 (3444)	5 (2)	3394 (3443)	10 (1)	3385 (3439)	4 (2)
		3417	15	3409 (3445)	36 (0)	3395 (3443)	64 (0)	3386 (3439)	115 (0)
	C−H stretching of rim H−C═C−H	3232	5	3252 (3237)	0 (0)	3251 (3228)	0 (0)	3250 (3224)	0 (1)
		3256	10	3273 (3259)	1 (1)	3272 (3250)	1 (1)	3271 (3247)	1 (2)
		3256	23	3273 (3259)	0 (1)	3272 (3250)	1 (3)	3272 (3247)	2 (6)
***anti*-3NH**	M^+-central benzene ring intermolecular stretching			350 (405)	83 (68)	195 (200)	30 (21)	154 (150)	24 (19)
	N−H stretching of bridge NH	3413	12	3436 (3461)	4 (0)	3427 (3457)	1 (0)	3428 (3450)	0 (1)
		3413	2	3436 (3461)	1 (4)	3427 (3457)	1 (2)	3428 (3450)	0 (0)
	C−H stretching of rim H−C═C−H	3219	8	3244 (3225)	0 (0)	3243 (3215)	0 (1)	3240 (3211)	0 (2)
		3244	11	3265 (3248)	2 (1)	3264 (3238)	3 (2)	3262 (3235)	3 (3)
		3244	33	3266 (3248)	1 (3)	3264 (3239)	1 (7)	3262 (3235)	2 (12)

[a] The values for the metal ion complexes with bottom and top faces are given in plain and parentheses respectively.

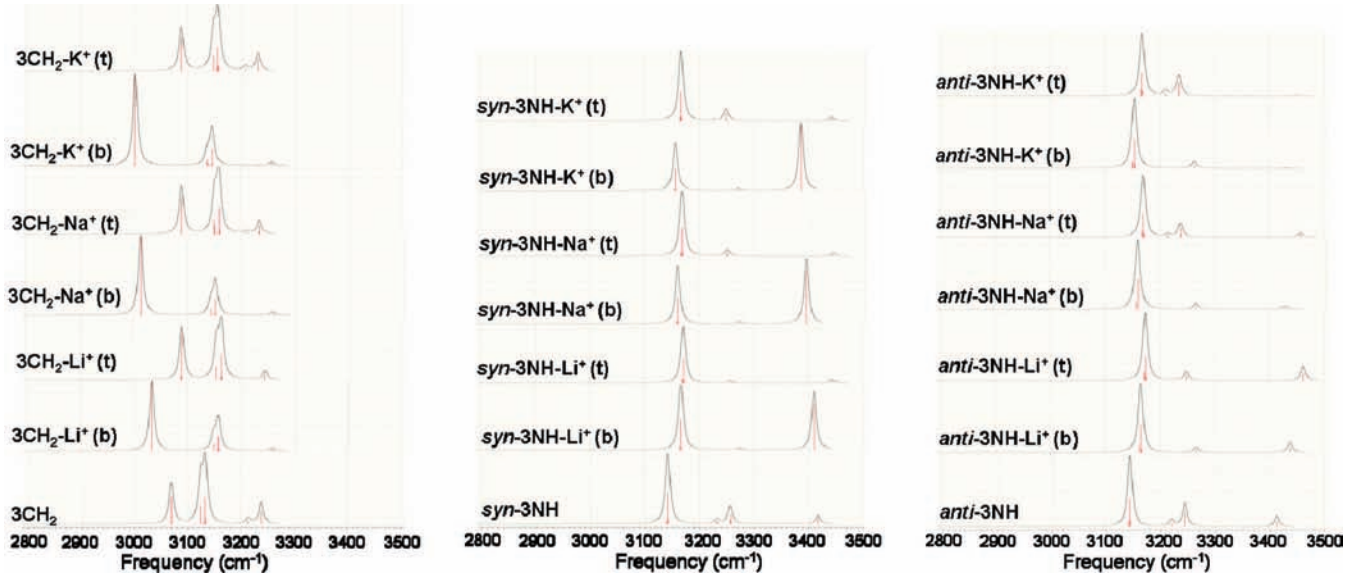

Figure 6. Peaks of vibrational frequencies (cm^{-1}) corresponding to C−H and N−H stretching modes lie in the range of 2800−3500 cm^{-1} for the cup-shaped molecules and their complexes with alkali metal cations of Li^+, Na^+, and K^+.

This explains stronger binding affinity of metal ions with the former than with the latter species. The molecular electrostatic potential surface of ***anti*-3NH** (view from bottom) shows a strongly negative potential due to the contributions of electron density from the central benzene ring and the three lone pair electrons of nitrogen. Therefore, the bottom side of ***anti*-3NH** exhibits the strongest binding affinity among different ligands considered in this study. We can observe the least electron density at the central benzene ring of ***syn*-3NH** (view from bottom) and also three highly positive regions due to the electropositive hydrogen atoms of N−H bridges, which undergo strong repulsive interactions with cations. The least electron density in the bottom cavity of ***syn*-3NH** indicates substantially low binding affinity (even lower than for benzene) for the metal ion binding to this bottom face. In the case of **$3CH_2$** and ***syn*-3NH**, the top face exhibits higher negative potential than the bottom face because of the contribution from three rim C═C bonds. Hence, the metal ions prefer top face over bottom face of these two ligands. The face preference is opposite in ***anti*-3NH** due to the participation of lone pair of electrons of nitrogen atoms. The present study reveals that the molecular electrostatic potential surfaces represent useful qualitative guide in predicting the cavity selectivity for metal ion binding with the cup-shaped molecules.

Vibrational Frequency Analysis

Frequency calculations performed at the B3LYP/6-31G(d) level confirm that all of the ligands and complexes are minima on their respective potential energy surfaces. Vibrational spectra can be useful to probe cation−π interactions. Hence, we have analyzed selected vibrational frequencies of the host molecules and complexes. As shown in Figure 5, the intermolecular stretching frequency ($\nu_{\text{ring centroid-M+}}$) in the complexes involving **1**, **$2CH_2$**, and **2NH** decreases as the metal ion size increases, and this is in accord with the binding strength of metal ion that follows $Li^+ > Na^+ > K^+$. It should be noted that two $\nu_{\text{ring centroid-M+}}$ stretching frequencies were observed in the complexes

involving **2CH$_2$**. Considering the higher frequency values for the complexes of **2CH$_2$**, there is a good correlation between the binding strength and intermolecular stretching frequency for systems **1**, **2CH$_2$**, and **2NH**.

The C−H and N−H bond lengths, which are closely associated with the metal ion interactions, obtained at the B3LYP/6-31G(d) level are provided in Table 3. Important vibrational frequencies obtained at the B3LYP/6-31G(d) level for the cup-shaped ligands and their metal ion bound complexes are given in Table 4. These frequencies will be useful for experimentalists to characterize bottom and top face complexes. All frequencies along with their intensities and symmetry for all of the ligands and complexes are provided in the Supporting Information. The data provided in Table 4 show that the stretching frequency between the metal ion and ring centroid of the cup-shaped molecules decreases as the atomic radius of metal ion increases. This is in correlation with the binding affinity of metal ions as $Li^+ > Na^+ > K^+$. In the case of binding of Li^+ and Na^+ with **3CH$_2$**, the bottom face complex exhibits notably higher $\nu_{\text{ring centroid-M+}}$ stretching frequency than the top face complex, whereas it is difficult to distinguish bottom and top face complexes based on this frequency mode alone for the binding of K^+. For the binding of Li^+ with ***anti*-3NH**, the $\nu_{\text{ring centroid-M+}}$ stretching frequency for the bottom face complex is about 55 cm^{-1} smaller compared to the top face complex. This can be attributed to the strong interactions of Li^+ with the three lone pair electrons of nitrogen atoms. The peaks obtained in the region of 2800−3500 cm^{-1} for the cup-shaped molecules and their complexes are depicted in Figure 6.

The metal ion complexation to the bottom face of **3CH$_2$** leads to weakening of endo C−H bond. This weakening is accompanied by bond elongation (Table 3) and a concomitant decrease of the vibrational frequency of endo C−H compared to the bare ligand (the frequency at around 3070 cm^{-1}, Figure 6 and Table 4). Figure 6 displays that the frequency of endo C−H of **3CH$_2$** at 3068 cm^{-1} is red-shifted by ∼37 (Li^+), 56 (Na^+), and 66 (K^+) cm^{-1} in the complexes. Furthermore, the intensity corresponding to this peak is very high in the complex and the intensity increases with increasing metal ion size. This is very important infrared (IR) spectral signature in identifying the metal ion complexation with the bottom face of **3CH$_2$**. The metal ion binding with the bottom face of **3CH$_2$** affects the noninteracting exo C−H and rim C−H bonds to a slight contraction (Table 3), and their stretching frequencies are blue-shifted compared to the corresponding frequencies of the bare ligand. It is interesting to note that the rim C−H stretch bands at 3213 and 3238 cm^{-1} for **3CH$_2$** are somewhat blue-shifted when Li^+ interacts with the top face, while they are red-shifted for Na^+ and K^+ complexes. A very similar situation is observed in the case of metal ion binding with the top face of ***syn*-** and ***anti*-3NH**. For the metal ion binding with the top face of **3CH$_2$**, the band of rim C−H stretch vibration of bare ligand is diminishing for Li^+ complex since smaller Li^+ ion fits inside the top cavity and appears to have insignificant interaction with the rim C−H bond, but it resembles that of bare ligand for Na^+ and K^+ complexes.

The N−H stretching frequency is observed around 3400 cm^{-1} for ***syn*-** and ***anti*-3NH**. Metal ion complexation with the bottom face of ***syn*-3NH** has significant influence on the N−H stretching frequency of the ligand. The N−H stretching frequency of ***syn*-3NH** at 3417 cm^{-1} is red-shifted by ∼10, 20, and 30 cm^{-1} with increasing intensity in Li^+, Na^+, and K^+ complexes, respectively. This red shift is due to the repulsive interaction between the metal ion and the N−H bonds. It should be noted that the N−H bond lengths are almost same or slightly elongated in the complexes compared to those in the ligand ***syn*-3NH**. For the metal ion complexation with the top face of ***syn*-** and ***anti*-3NH**, the N−H stretching frequency is almost vanished despite it is blue-shifted with respect to bare ligand. The rim C−H stretching frequencies of ***syn*-3NH** observed at 3232 and 3256 cm^{-1} seem to disappear in Li^+ bound top face complex, while they gradually appear at lower frequency for the corresponding Na^+ and K^+ complexes. The present study indicates that vibrational spectra will be helpful to characterize different alkali metal ion complexation with the ring fused benzenes. Further, they will assist to distinguish top and bottom face complexes.

Conclusions

The present paper reports a comprehensive theoretical study of the interactions of alkali metal ions (Li^+, Na^+, and K^+) with the planar and cup-shaped ring fused benzenes. Similar to benzene, the C−C bonds of the central hexagon in the ring fused benzenes undergo elongation upon complexation with the alkali metal ions. The degree of bond alternation is much higher in the cup-shaped molecules and their metal ion complexes compared to **2CH$_2$**, **2NH** and their metal ion complexes. The binding affinity of metal ion with the ligands under the study follows the order: $Li^+ > Na^+ > K^+$. Metal ions prefer to bind with the top face rather than bottom face of ligands **3CH$_2$** and ***syn*-3NH**. In contrast, the bottom face is more favorable over top face for the metal ion binding with ***anti*-3NH** because of the strong interactions of lone pair electrons of three nitrogen atoms with the metal ion, in addition to the cation−π interaction. Multiple weak, nonoptimal cation−π (by rim C═C bonds) interactions contribute significantly to the overall binding strength of the metal ion interacting with the top face of the cup-shaped molecules. The extent of electron charge transfer from ligand to metal ion is larger for the cup-shaped molecules than the planar compounds. The present study reveals that the molecular electrostatic potential surfaces are a useful qualitative guide in predicting the cavity selectivity for metal ion binding with the cup-shaped molecules. Vibrational spectra obtained in the region 2800−3500 cm^{-1} for the cup-shaped molecules and their complexes exhibit some characteristic spectral signatures that could assist in distinguishing top and bottom face complexes involving different metal ions. This type of computational understanding allows chemists to control the geometry of the complexes and to design precisely complementary hosts for a given guest.

Acknowledgment. This work was supported by the National Science Foundation (NSF) through CREST Grant HRD-0318519 and Office of Naval Research (ONR) Grant N00034-03-1-0116. Mississippi Center for Supercomputing Research (MCSR) is acknowledged for generous computational facilities. We thank Mr. A. Hassan for his help in making some of the molecular electrostatic potential pictures.

Supporting Information Available: Total energies, BSSE correction, the interaction energies, and the extent of charge transfer from ligand to metal ion obtained at the B3LYP/6-31G(d), MP2/6-31G(d) and MP2(FULL)/6-311+G(d,p)//MP2/6-31G(d) levels; MP2/6-31G(d) level optimized Cartesian coordinates and the vibrational frequencies obtained at the B3LYP/6-31G(d) level. This material is available free of charge via the Internet at http://pubs.acs.org.

References and Notes

(1) Dougherty, D. A. *Science* **1996**, *271*, 163.
(2) Ma, J. C.; Dougherty, D. A. *Chem. Rev.* **1997**, *97*, 1303.

(3) (a) Yoon, J.; Kim, S. K.; Singh, N. J.; Kim, K. S. *Chem. Soc. Rev.* **2006**, *35*, 355. (b) Meyer, E. A.; Castellano, R. K.; Diederich, F. *Angew. Chem., Int. Ed.* **2003**, *42*, 1210. (c) Lopinski, G. P.; Wayner, D. D. M.; Wolkow, R. A. *Nature* **2000**, *406*, 48. (d) Weber, G. *Protein interactions*; Chapman & Hall: London, 1992. (e) Jones, S.; Thornton, J. M. *Proc. Natl. Acad. Sci. U.S.A.* **1996**, *93*, 13.

(4) Kim, K. S.; Tarakeshwar, P.; Lee, J. Y. *Chem. Rev.* **2000**, *100*, 4145.

(5) Zarić, S. D.; Popović, D. M.; Knapp, E.-W. *Chem. Eur. J.* **2000**, *6*, 3935.

(6) (a) Gallivan, J. P.; Dougherty, D. A. *J. Am. Chem. Soc.* **2000**, *122*, 870. (b) Mecozzi, S.; West, A. P., Jr.; Dougherty, D. A. *Proc. Natl. Acad. Sci. U.S.A.* **1996**, *93*, 10566. (c) Mecozzi, S.; West, A. P., Jr.; Dougherty, D. A. *J. Am. Chem. Soc.* **1996**, *118*, 2307.

(7) (a) Gallivan, J. P.; Dougherty, D. A. *Proc. Natl. Acad. Sci. U.S.A.* **1999**, *96*, 9459. (b) Gallivan, J. P.; Dougherty, D. A. *Org. Lett.* **1999**, *1*, 103. (c) Ngola, S. M.; Dougherty, D. A. *J. Org. Chem.* **1998**, *63*, 4566. (d) Coates, G. W.; Dunn, A. R.; Henling, L. M.; Dougherty, D. A.; Grubbs, R. H. *Angew. Chem., Int. Ed. Engl.* **1997**, *36*, 248.

(8) (a) Pellequer, J. -L.; Zhao, B.; Kao, H. -I.; Bell, C. W.; Li, K.; Li, Q. X.; Karu, A. E.; Roberts, V. A. *J. Mol. Biol.* **2000**, *302*, 691. (b) Kua, J.; Zhang, Y.; McCammon, J. A. *J. Am. Chem. Soc.* **2002**, *124*, 8260. (c) Fukin, G. K.; Lindeman, S. V.; Kochi, J. K. *J. Am. Chem. Soc.* **2002**, *124*, 8329. (d) Thomas, K. J.; Sunoj, R. B.; Chandrasekhar, J.; Ramamurthy, V. *Langmuir* **2000**, *16*, 4912.

(9) (a) Wintjens, R.; Liévin, J.; Rooman, M.; Buisine, E. *J. Mol. Biol.* **2000**, *302*, 395. (b) Tan, J. X.; Jiang, H. L.; Zhu, W. L.; Chen, K. X.; Ji, R. Y. *J. Chem. Soc., Perkin Trans. 2* **1998**, *1*, 1. (c) Harrison, R. G.; Fox, O. D.; Meng, M. O.; Dalley, N. K.; Barbour, L. J. *Inorg. Chem.* **2002**, *41*, 838.

(10) (a) Woodin, R. L.; Beauchamp, J. L. *J. Am. Chem. Soc.* **1978**, *100*, 501. (b) Sunner, J.; Nishizawa, K.; Kebarle, P. *J. Phys. Chem.* **1981**, *85*, 1814. (c) Deakyne, C. A.; Meot-ner, M. *J. Am. Chem. Soc.* **1985**, *107*, 474. (d) Meot-ner, M.; Deakyne, C. A. *J. Am. Chem. Soc.* **1985**, *107*, 469.

(11) (a) Amunugama, R.; Rodgers, M. T. *Int. J. Mass Spectrom.* **2003**, *227*, 339. (b) Koyanagi, G. K.; Bohme, D. K. *Int. J. Mass Spectrom.* **2003**, *227*, 563.

(12) Hunter, C. A.; Low, C. M. R.; Rotger, C.; Vinter, J. G.; Zonta, C. *Proc. Natl. Acad. Sci. U.S.A.* **2002**, *99*, 4873.

(13) Kim, D.; Lee, E. C.; Kim, K. S.; Tarakeshwar, P. *J. Phys. Chem. A* **2007**, *111*, 7980.

(14) Kim, D.; Hu, S.; Tarakeshwar, P.; Kim, K. S.; Lisy, J. M. *J. Phys. Chem. A* **2003**, *107*, 1228.

(15) Vijay, D.; Sastry, G. N. *J. Phys. Chem. A* **2006**, *110*, 10148.

(16) (a) Reddy, A. S.; Vijay, D.; Sastry, G. M.; Sastry, G. N. *J. Phys. Chem. B* **2006**, *110*, 2479. (b) Reddy, A. S.; Vijay, D.; Sastry, G. M.; Sastry, G. N. *J. Phys. Chem. B* **2006**, *110*, 10206.

(17) Reddy, A. S.; Zipse, H.; Sastry, G. N. *J. Phys. Chem. B* **2007**, *111*, 11546.

(18) Reddy, A. S.; Sastry, G. N. *J. Phys. Chem. A* **2005**, *109*, 8893.

(19) Ruan, C.; Rodgers, M. T. *J. Am. Chem. Soc.* **2004**, *126*, 14600.

(20) Choi, H. S.; Suh, S. B.; Cho, S. J.; Kim, K. S. *Proc. Natl. Acad. Sci. U.S.A.* **1998**, *95*, 12094.

(21) Kim, J.; Kim, Y. K.; Park, N.; Hahn, J. H.; Ahn, K. H. *J. Org. Chem.* **2005**, *70*, 7087.

(22) Tu, C.; Liu, D.; Surowiec, K.; Purkiss, D. W.; Bartsch, R. A. *Org. Biomol. Chem.* **2006**, *4*, 2938.

(23) Zonta, C.; Cossu, S.; De Lucchi, O. *Eur. J. Org. Chem.* **2000**, 1965.

(24) Armentrout, P. B.; Rodgers, M. T. *J. Phys. Chem. A* **2000**, *104*, 2238.

(25) Amicangelo, J. C.; Armentrout, P. B. *J. Phys. Chem. A* **2000**, *104*, 11420.

(26) (a) Amunugama, R.; Rodgers, M. T. *J. Phys. Chem. A* **2002**, *106*, 5529. (b) Amunugama, R.; Rodgers, M. T. *J. Phys. Chem. A* **2002**, *106*, 9092. (c) Amunugama, R.; Rodgers, M. T. *J. Phys. Chem. A* **2002**, *106*, 9718. (d) Amunugama, R.; Rodgers, M. T. *Int. J. Mass Spectrom.* **2003**, *222*, 431. (e) Ryzhov, V.; Dunbar, R. C.; Cerda, B.; Wesdemiotis, C. *J. Am. Soc. Mass. Spectrom.* **2000**, *11*, 1037.

(27) Gapeev, A.; Yang, C.-Y.; Klippenstein, S. J.; Dunbar, R. C. *J. Phys. Chem. A* **2000**, *104*, 3246.

(28) Tsuzuki, S.; Yoshida, M.; Uchimaru, T.; Mikami, M. *J. Phys. Chem. A* **2001**, *105*, 769.

(29) Vijay, D.; Sastry, G. N. *Phys. Chem. Chem. Phys.* **2008**, *10*, 582.

(30) ois Gal, J.-F.; Maria, P.-C.; Decouzon, M.; Mo, O.; Yánez, M.; Abboud, J. L. M. *J. Am. Chem. Soc.* **2003**, *125*, 10394.

(31) Amunugama, R.; Rodgers, M. T. *Int. J. Mass Spectrom.* **2003**, *227*, 1.

(32) Ikuta, S. *J. Mol. Struct. (THEOCHEM)* **2000**, *530*, 201.

(33) Dunbar, R. C. *J. Phys. Chem. A* **2002**, *106*, 9809.

(34) Priyakumar, U. D.; Punnagai, M.; Mohan, G. P. K.; Sastry, G. N. *Tetrahedron* **2004**, *60*, 3037.

(35) Macias, A. T.; Norton, J. E.; Evanseck, J. D. *J. Am. Chem. Soc.* **2003**, *125*, 2351.

(36) (a) Dijkstra, P. J.; Brunink, J. A.; Bugge, K.-E.; Reinhoudt, D. N.; Harkema, S.; Ungaro, R.; Ugozzoli, F.; Ghidini, E. *J. Am. Chem. Soc.* **1989**, *111*, 7567. (b) Zhou, H.; Surowiec, K.; Purkiss, D. W.; Bartsch, R. A. *Org. Biomol. Chem.* **2005**, *3*, 1676.

(37) (a) Siegel, J. S. *Angew. Chem., Int. Ed. Engl.* **1994**, *33*, 1721. (b) Frank, N. L.; Baldridge, K. K.; Gantzel, P.; Siegel, J. S. *Tetrahedron Lett.* **1995**, *36*, 4389. (c) Buergi, H.-B.; Baldridge, K. K.; Hardcastle, K.; Frank, N. L.; Gantzel, P.; Siegel, J. S.; Ziller, J. *Angew. Chem., Int. Ed. Engl.* **1995**, *34*, 1454. (d) Frank, N. L.; Baldridge, K. K.; Siegel, J. S. *J. Am. Chem. Soc.* **1995**, *117*, 2102.

(38) Zonta, C.; Fabris, F.; De Lucchi, O. *Org. Lett.* **2005**, *7*, 1003.

(39) Hassan, A.; Dinadayalane, T. C.; Leszczynski, J. *Chem. Phys. Lett.* **2007**, *443*, 205.

(40) (a) Becke, A. D. *Phys. Rev. A* **1988**, *38*, 3098. (b) Lee, C.; Yang, W.; Parr, R. G. *Phys. Rev. B* **1988**, *37*, 785.

(41) Møller, C.; Plesset, M. S. *Phys. Rev.* **1934**, *46*, 618.

(42) Boys, S. F.; Bernardi, F. *Mol. Phys.* **1970**, *19*, 553.

(43) GaussView, Version 3.09, Dennington II; Keith, R.; Millam, T.; Eppinnett, J.; Hovell, K.; Gilliland, W. L.; Semichem, R., Inc., Shawnee Mission, KS, 2003.

(44) Frisch, M. J. ; Trucks, G. W.; Schlegel, H. B.; Scuseria, G. E.; Robb, M. A.; Cheeseman, J. R.; Montgomery Jr., J. A.; Vreven, T.; Kudin, K. N.; Burant, J. C.; Millam, J. M.; Iyengar, S. S.; Tomasi, J.; Barone, V.; Mennucci, B.; Cossi, M.; Scalmani, G.; Rega, N.; Petersson, G. A.; Nakatsuji, H.; Hada, M.; Ehara, M.; Toyota, K.; Fukuda, R.; Hasegawa, J.; Ishida, M.; Nakajima, T.; Honda, Y.; Kitao, O.; Nakai, H.; Klene, M.; Li, X.; Knox, J. E.; Hratchian, H. P.; Cross, J. B.; Adamo, C.; Jaramillo, J.; Gomperts, R.; Stratmann, R. E.; Yazyev, O.; Austin, A. J.; Cammi, R.; Pomelli, C.; Ochterski, J. W.; Ayala, P. Y.; Morokuma, K.; Voth, G. A.; Salvador, P.; Dannenberg, J. J.; Zakrzewski, V. G.; Dapprich, S.; Daniels, A. D.; Strain, M. C.; Farkas, O.; Malick, D. K.; Rabuck, A. D.; Raghavachari, K.; Foresman, J. B.; Ortiz, J. V.; Cui, Q.; Baboul, A. G.; Clifford, S.; Cioslowski, J.; Stefanov, B. B.; Liu, G.; Liashenko, A.; Piskorz, P.; Komaromi, I.; Martin, R. L.; Fox, D. J.; Keith, T.; Al-Laham, M. A.; Peng, C. Y.; Nanayakkara, A.; Challacombe, M.; Gill, P. M. W.; Johnson, B.; Chen, W.; Wong, M. W.; Gonzalez, C.; Pople, J. A. *Gaussian 03*, revision C.02; Gaussian, Inc.: Wallingford CT, 2004.

(45) Haddon, R. C. *J. Phys. Chem. A* **2001**, *105*, 4164.

(46) Haddon, R. C. POAV3: Release 3.0, 1993.

(47) Mills, W. H.; Nixon, I. G. *J. Chem. Soc.* **1930**, 2510.

(48) Nicholas, J. B.; Hay, B. P.; Dixon, D. A. *J. Phys. Chem. A* **1999**, *103*, 1394.

(49) Rathore, R.; Lindeman, S. V.; Kumar, A. S.; Kochi, J. K. *J. Am. Chem. Soc.* **1998**, *120*, 6012.

(50) (a) Quinn, D. M.; Feaster, S. R.; Nair, H. K.; Baker, N. A.; Radić, Z.; Taylor, P. *J. Am. Chem. Soc.* **2000**, *122*, 2975. (b) Mo, Y.; Subramanian, G.; Gao, J.; Ferguson, D. M. *J. Am. Chem. Soc.* **2002**, *124*, 4832.

(51) Kamieth, M.; Klärner, F.-G.; Diederich, F. *Angew. Chem., Int. Ed.* **1998**, *37*, 3303.

JP802236K